

# A Novel Asterisk-Shaped Circularly Polarized RFID Tag for On-Metal Applications

Umar H. Khan<sup>1</sup>, Bilal Aslam<sup>1</sup>, Javaria Khan<sup>1</sup>, Misha Nadeem<sup>1</sup>, Humayun Shahid<sup>1</sup>,  
Muhammad Awais Azam<sup>1</sup>, Yasar Amin<sup>1,2</sup>, and Hannu Tenhunen<sup>2</sup>

<sup>1</sup> ACTSENA Research Group  
University of Engineering and Technology, 47050-Taxila, Pakistan  
umar.hasan@uettaxila.edu.pk

<sup>2</sup> iPack VINN Excellence Center  
Royal Institute of Technology, SE-16440, Stockholm, Sweden  
{yasr, hannu}@kth.se

**Abstract** — An asterisk-shaped, metal-mountable RFID tag with a minuscule footprint is presented. The proposed design makes use of multiple asymmetric slots patterned in a cross-shaped fashion to achieve circular polarization. The structure is excited capacitively using a terminally-grounded, T-shaped feed line positioned within the slots. This peculiar arrangement permits the attainment of circular polarized radiation characteristics over a wide band of operation. Impedance matching, antenna size reduction and read range enhancement are the additional advantages offered by the embedded feed line. The final design is realized on a commercially available FR-4 substrate over dimensions of 40 x 40 mm<sup>2</sup> yielding an impedance bandwidth and an axial ratio bandwidth of 37 MHz and 20 MHz, respectively. Improvement in antenna gain (and consequently in the read range) is reported upon mounting the tag on metallic surfaces.

**Index Terms** — Circular polarization, impedance matching, Radio Frequency Identification (RFID).

## I. INTRODUCTION

Applications built upon radio frequency identification (RFID) technology, particularly the ones in the ultra high frequency (UHF) band of operation (860-960 MHz), have increased in number dramatically over the last decade [1-4]. This primarily is due to a number of advantages associated with RFID tags operating in the UHF band including enhanced read range, high data transfer rate, and small tag footprint [5-8]. For most practical applications, a hefty majority of the RFID reader antennas that exist today incorporate circularly polarized radiation characteristics. Doing so offers a multitude of benefits such as an increase in orientation diversity and reduction in polarization

mismatch loss. Most of the commercially available tag antennas, however, are linearly polarized, causing a stark mismatch in polarization between the reader and the tag antenna. This polarization mismatch translates to an undesirable decrease in the tag's read range, limiting the overall performance of any application-specific RFID system within which the tag is deployed [9, 10]. Doing away with the polarization mismatch is bound to result in enhanced read range and tag-orientation independence, making it a highly sought feature. Owing to these advantages, designing RFID tag antennas with circularly polarized radiation characteristics that persist over a wide band of operation has been the prime focus of recent research effort [11, 12].

Yet another sought-after feature for RFID tags is the capability of being readily mountable on metallic surfaces. The majority of metal-mountable RFID tags are linearly polarized in nature [13-17], falling prey to polarization mismatch loss and depriving the RFID system of orientation-independence characteristics. There are but only a few RFID tag antennas reported in literature that both operate in the UHF band and possess circularly polarized radiation characteristics [18, 19]. Moreover, for RFID tags that incorporate circularly polarized radiation characteristics, are metal-mountable, and operate in the UHF band, the structures deployed for providing the feed are essentially located outside the radiating components [20, 21]. This arrangement results in an overall increase in the tag antenna's size. In addition, feeding networks realized external to the radiators generally translate to structural asymmetries that are manifested in the design of the tag antenna. This, in turn, leads to a decrease in the antenna's boresight gain. Lin et al. [22] have presented a RFID reader antenna that incorporates a feeding network embedded within the radiating elements, operates in the circularly

polarized mode, and offers a wide axial ratio bandwidth equal to 12 MHz. The antenna, however, has been tuned to match an impedance of  $50\Omega$  and has its thickness exceeding 10 mm. These drawbacks render an antenna of this type unfit for deployment in modern-day, unobtrusive RFID applications

In this paper, a compact RFID tag operating in the UHF band with circularly polarized radiation characteristics. Opting in for a peculiar asterisk-shaped patch design offers advantages such as miniscule tag footprint and an appreciably wide 3 dB axial ratio bandwidth. The tag not only offers benefits such as orientation independence and enhanced read range, but also boasts the sought-after feature of being readily mountable on metallic surfaces. The tag antenna is fabricated on readily available substrate and the simulated electromagnetic characteristics are juxtaposed with the experimental findings.

## II. ANTENNA DESIGN

The flowchart in Fig. 1 elaborates the systematic approach that has been adhered to during the antenna design process.

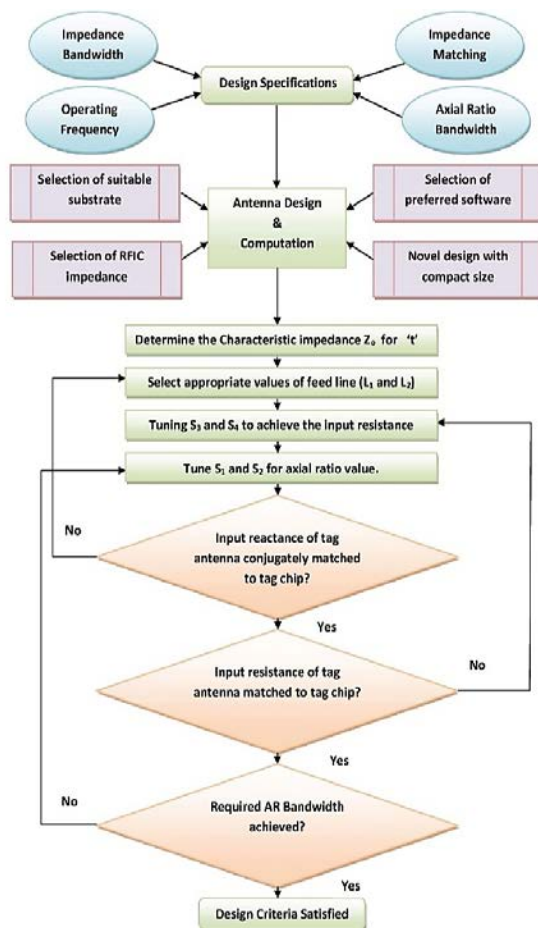


Fig. 1. Flow chart of the proposed antenna design.

The detailed layout of the formulated RFID tag boasting circularly polarized radiation characteristics is depicted in Fig. 2. An asterisk-shaped patch antenna of dimensions  $40 \times 40 \text{ mm}^2$  is realized on an FR-4 substrate that has a thickness of 1.6 mm. Selecting this particular patch design allows for reduction in tag antenna size and also facilitates in maintaining the desired axial ratio over a wide band of operation. Four asymmetric slots, labeled as  $S_1$  through  $S_4$ , are meticulously etched within the asterisk-shaped patch to not only achieve circularly polarized radiation characteristics, but also to ensure impedance match between the antenna structure and the Radio Frequency Integrated Circuit (RF IC). In particular, slots  $S_1$  and  $S_2$  patterned in a cross-like fashion, are responsible for the attainment of circularly polarized radiation characteristics. Slots  $S_3$  and  $S_4$ , patterned in a plus-shaped manner and provided with feeding lines, allow for the impedance match to take place. The width of the asymmetric slots, with and without the feeding lines, are  $S_{w2}=4 \text{ mm}$  and  $S_{w1}=3.5 \text{ mm}$ , respectively. The L-shaped microstrip feed line is oriented at a coupling distance,  $D$ , around 1 mm from the radiating patch. The width of the main feed line,  $t$ , is 2 mm and is further divided into two unequal feed lines of lengths  $L_1$  and  $L_2$  with the RF IC in between. The formulated design, in its entirety, is fabricated on a ground plane having a size of  $60 \times 60 \text{ mm}^2$ .

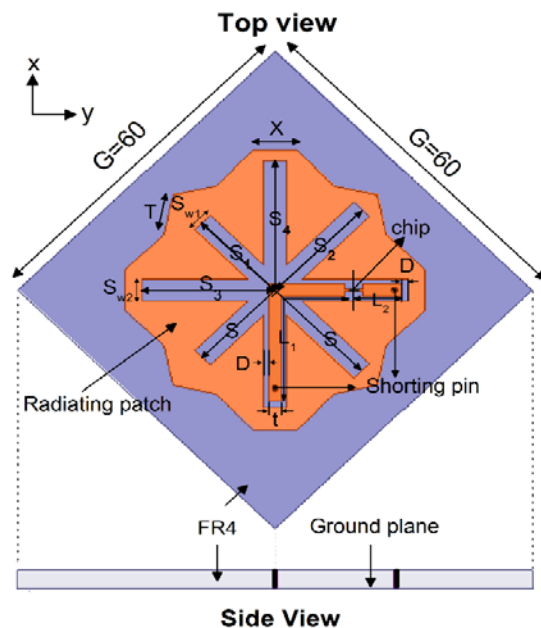


Fig. 2. Geometry of the proposed CP RFID antenna design (Units: mm).

Designing for circularly polarized radiation characteristics involves varying the lengths of both the cross and plus-shaped slots incrementally and concurrently, such that the surface current density is

equally distributed over the entire patch, resulting in the generation of two orthogonal degenerated modes. The next step involves controlling the phase difference between the two degenerated modes. This is done by appropriate tuning of the length of  $S_1$  and length of  $S_2$ . When the length of  $S_1$  is less than that of  $S_2$ , the path of current in the x-direction will be longer than that for the y-direction. This difference in the lengths of  $S_1$  and  $S_2$  leads to the formation of lower and higher resonant modes. Careful selection of lengths of both  $S_1$  and  $S_2$  results in the two degenerate modes being out of phase by  $90^\circ$ , achieving right-hand circular polarization radiation. Similarly, rendering the length of  $S_2$  great than the length of  $S_1$  generates left-hand circular polarization radiation. The embedded nature of the slotted design allows for the overall antenna size to become minuscule.

The impedance matching phase lies at the core of the tag design process. The RF IC chosen for deployment in the formulated tag antenna is Alien Higgs that operates in the FCC band (902-928 MHz). The RF IC is connected between two feed lines as shown in Fig. 2, and has an associated value of impedance mounting to  $13 - j111 \Omega$  at an operating frequency of 915 MHz. In order to ensure that maximum amount of power gets transferred across from the tag antenna to the chip, the value of impedance for the tag antenna is tuned to be around  $13 + j111 \Omega$  at 915 MHz. The real part of the antenna's impedance is adjusted by varying the lengths of  $S_1$  and  $S_2$ , whereas the required value of inductive reactance is achieved by dint of a pair of short-circuited microstrip transmission lines oriented in the etched slots.

The calculation for length of the short-circuited microstrip lines  $L_1$  and  $L_2$  follows from transmission line theory [23, 24]:

$$111 = Z_o \tan\left[\frac{2\pi}{\lambda}(L_1 + L_2)\right], \quad (1)$$

$$Z_o = \frac{120}{\sqrt{\epsilon_{eff}}} \frac{1}{\left\{\left(\frac{w}{h}\right) + 1.393 + 0.677\right\} \left\{\ln\left(\frac{w}{h}\right) + 1.444\right\}}}, \quad (2)$$

$$\epsilon_{eff} = \frac{\epsilon_r + 1}{2} + \frac{\epsilon_r - 1}{2} \times \left\{ \frac{1}{\sqrt{1 + \frac{12h}{w}}} \right\}, \quad (3)$$

where  $Z_o$  equals the characteristic impedance of a short-circuited line and  $\lambda$  represents the guided wavelength at 915 MHz. Plugging in the relevant values for  $Z_o$  and  $\lambda$ , the total length of the transmission line,  $L_1 + L_2$ , turns out to be 36 mm. While many solutions exist for solving the equation  $L_1 + L_2 = 36$  mm, the values are chosen such that  $L_1$  approximately equals to  $L_2 + \lambda/6$ . Owing to slight drift in the impedance value of the RF IC as compared to the one quoted on the datasheet, the best impedance match is attained when total length  $L_1 + L_2$  equals 37.7 mm. In addition to impedance matching, this peculiar arrangement also offers the advantage of tag miniaturization. The design parameters are optimized using full-wave simulation tool HFSS<sup>TM</sup>, and are shown in Table 1.

Table 1: Optimized design parameters (length) of the tag

Parameters	$S_1$	$S_2$	$S_3$	$S_4$	$S_5$
( $\lambda$ )	0.052	0.062	0.067	0.069	0.011
Parameters	$L_1$	$L_2$	T	X	S
( $\lambda$ )	0.095	0.019	0.022	0.021	0.113

### III. RESULTS AND DISCUSSION

The design of the formulated RFID tag antenna has been fine-tuned by thoroughly examining various key electromagnetic descriptors in an iterative fashion. The investigation is orchestrated using full wave electromagnetic design tool HFSS<sup>TM</sup>. The meticulously refined design is realized on an FR-4 substrate as shown in Fig. 3.

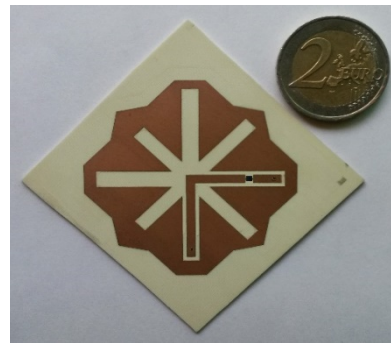


Fig. 3. Fabricated RFID tag antenna.

The fabricated tag prototype is scrutinized for its performance experimentally. The input impedance of the tag antenna is measured by two-port differential probe measurement method, as in [25, 26], using Vector Network Analyzer (MS2026B, Anritsu). The findings for the impedance measurement are depicted in Fig. 4.

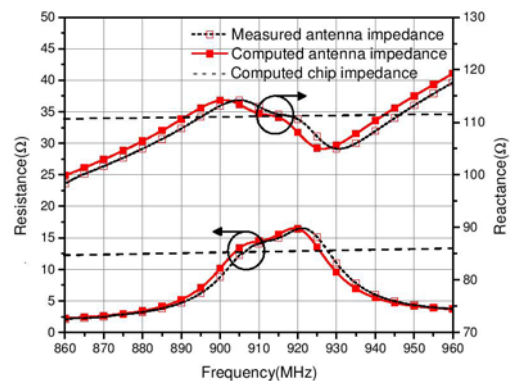


Fig. 4. Measured and computed impedances of the proposed antenna.

It can be observed that the impedance of the RF IC varies only slightly with a change in the frequency. The

resistance and reactance of the tag antenna exhibit a close conjugate match with the RF IC's impedance at 915 MHz. The computed and measured return loss is illustrated in Fig. 5. The measured return loss is calculated using the measured antenna impedance. A 10 dB return loss bandwidth equal to 37 MHz (897–934 MHz) has been reported experimentally, making the proposed RFID tag compliant with the North American frequency band. The computed values and measured results for impedance measurement and return loss are, principally, in good accord with one another.

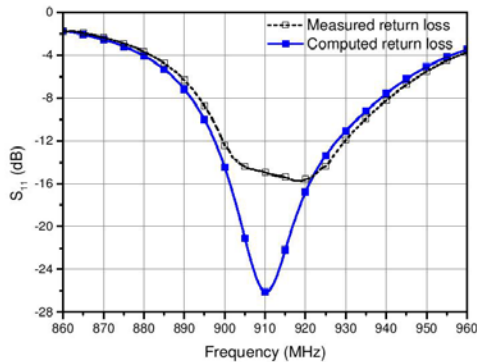


Fig. 5. Measured and computed return loss of the proposed antenna.

The effect of varying the length of the feedline and the asterisk-shaped slot on circular polarization bandwidth is investigated. Embedding the capacitively coupled feed lines, namely  $L_1$  and  $L_2$ , within the asterisk-shaped slots translates to a significant phase delay being induced that contributes towards cross-polarized excitation. To ensure resonant modes centered about 915 MHz, appropriate slot lengths have been chosen after exhaustive comparison of two scenarios: length of  $S_1 <$  length of  $S_2$  (condition 1) and length of  $S_1 >$  length of  $S_2$  (condition 2).

After optimizing the design iteratively the associated axial ratio bandwidth of condition 1 (length of  $S_1=17$  mm, length of  $S_2=20.1$  mm) and condition 2 (length of  $S_1=21.8$  mm, length of  $S_2=15.7$  mm), as shown in Fig. 6, turns out to be 20 MHz for both the scenarios. The range of the axial ratio bandwidth for condition 1 is (899–919 MHz), and for condition 2 is (896–916 MHz).

The default choice, however, is the case where length of  $S_1 <$  length of  $S_2$  because, here, the axial ratio bandwidth lies within the FCC band of operation. The results for amplitude and phase along the boresight direction are illustrated in Figs. 7 (a) and (b), respectively.

From Fig. 7 (a), it can be observed that the  $|E_x|$  and  $|E_y|$  are equal in amplitude. Figure 7 (b) shows that for condition 1, a phase difference  $\Phi_x - \Phi_y = 90^\circ$  is observed at 915 MHz, which depicts right hand circular polarization. For condition 2, phase difference  $\Phi_y - \Phi_x = 90^\circ$  is noted at around 900 MHz, which signifies left hand circular

polarization. This validates the existence of appreciable circular polarization radiation characteristics at 915 MHz which is within the band of interest.

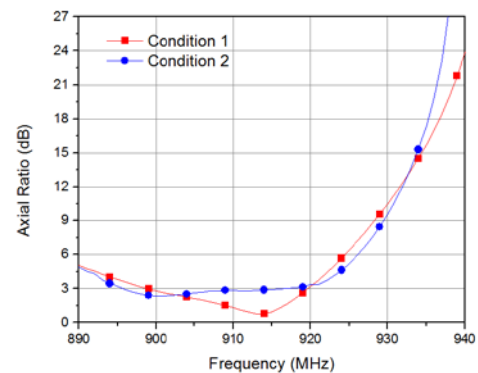


Fig. 6. Axial ratio of the proposed antenna design.

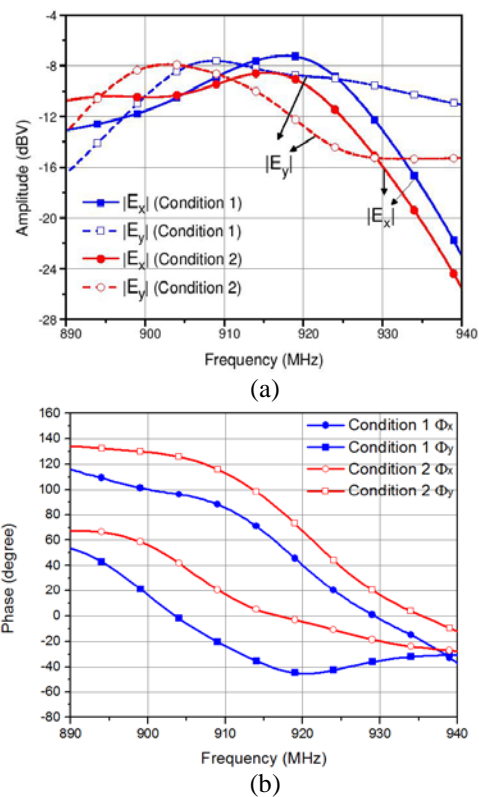


Fig. 7. Amplitude (a) and phase (b) diagrams of boresight radiation field  $E_x$  and  $E_y$ .

Circularly polarized radiation characteristics inherent with the tag antenna design are demonstrated by plotting the simulated surface current distribution at 915 MHz in Fig. 8. The figure depicts the changes in the surface current distribution and the direction of the distributed current at incremental time phases of  $0^\circ$ ,  $45^\circ$ ,  $90^\circ$  and  $135^\circ$ . The counterclockwise direction of the current

accompanied by an increase in the intensity of the same solidifies the existence of an RHCP-excited radiation in the design.

Since the input impedance of the formulated tag antenna has been conjugately matched with the impedance of the chip (and not to a 50Ω co-axial feedline) measuring the radiation pattern of the designed tag using conventional anechoic chamber setup is not possible. The results are delimited to the computed scenario only for both free-space and on-metal scenarios. Figure 9 shows the radiation pattern at 915 MHz.

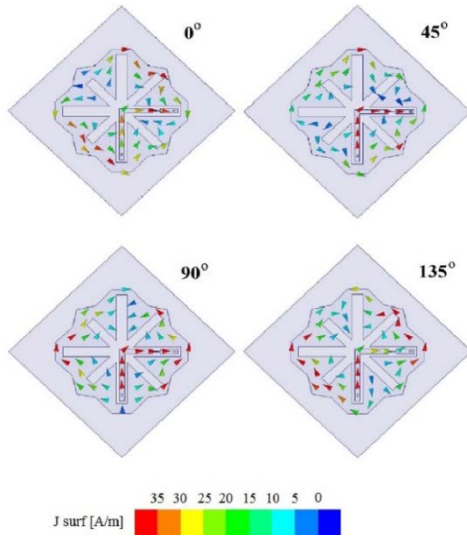


Fig. 8. Current distribution at 915 MHz.

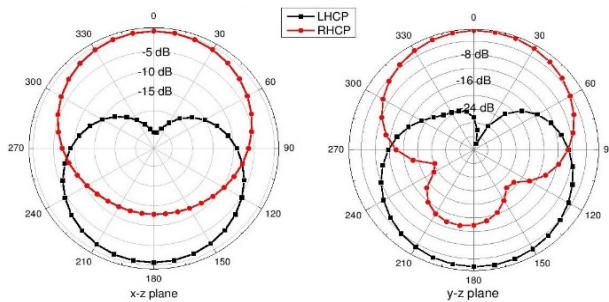


Fig. 9. Normalized CP gain radiation pattern at 915 MHz.

It is evident from Fig. 9 that, the formulated antenna boasts a 3-dB beam width of around 74° and an appreciable front-to-back radiation ratio in the order of 22 dB for both x-z and y-z planes. The appreciable front-to-back radiation ratio validates the existence of pure right-hand circularly polarized radiation characteristics exhibited in free space.

Figure 10 depicts the values of electric field strength in the azimuth and elevation plane obtained upon mounting the tag on a uniform metallic sheet of 400 x 400 mm<sup>2</sup>. The results show that the values of

E-theta and E-phi are almost identical, verifying the existence of circularly polarized radiation characteristics associated with the formulated tag even when the tag is mounted on the metal surface.

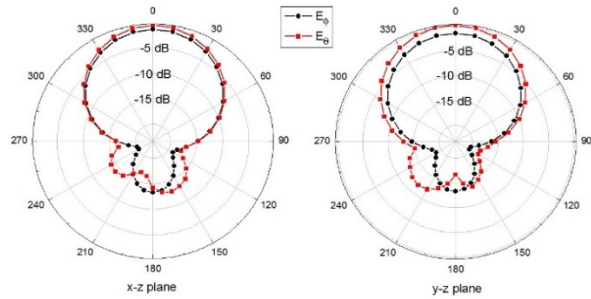


Fig. 10. Antenna realized gain radiation pattern on 400 x 400 mm<sup>2</sup> metallic plate.

The change in gain of the tag antenna upon deployment free space and metallic surfaces is computed. The gain is improved by a factor of 5 dB when the tag antenna is moved from free space on to a metallic surface. A larger metallic surface yields a larger area over which the antenna’s current is distributed, resulting in a larger overall gain. As seen in Fig. 11, for ground plane, sizes more than 100 x 100 mm<sup>2</sup>, the antenna gain remains well above -10.4 dBic. The calculated and measured read range of the proposed tag in free space and on metal plate sized 400 x 400 mm<sup>2</sup> is shown in Table 2 and measurement setup with Impinj™ RFID reader (xPortal) is shown in Fig. 12.

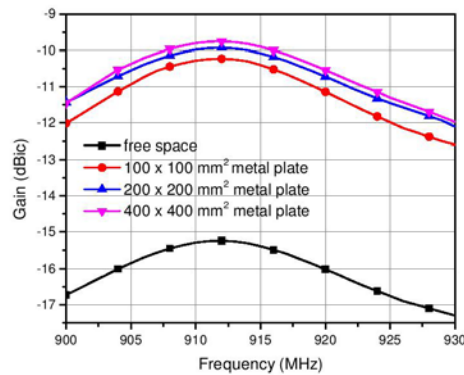


Fig. 11. Computed gain for different metal plate sizes at 915 MHz.

Table 2: Readrange of the proposed antenna with and without metal plate

Condition	Computed Gain (dBi)	Readrange Calculated	Readrange Measured
Free space	-15.3	1.94m	1.52m
On metal, 400x400mm <sup>2</sup>	-9.7	3.69m	3.36m



Fig. 12. Measurement setup for readrange.

From Table 3, it is evident that the proposed RFID tag antenna offers a significantly smaller footprint when stacked against designs presented in [20] and [21]. The decrease in size has been achieved without compromising on the gain of the tag antenna which, being  $-15.3$  dBi, is still comparable to competing designs. That said, the proposed tag offers an appreciably wide axial ratio bandwidth of 20 MHz, which is a clear improvement over designs reported in [20] and [21]. Similarly, the overall radiating size of  $40 \times 40 \text{ mm}^2$  has also been observed as being the minimum among the compared designs.

Table 3: Comparison of different antenna parameters

Antenna Ground Plane ( $\text{mm}^2$ )	Computed Gain (dBi)	AR Bandwidth (MHz)	Radiating Size ( $\text{mm}^2$ )
60x60 [pro]	-15.3	20	40x40
70x70 [21]	-14.4	6	50.5x50.5
80x80 [20]	-11.4	6	55.7x55.7

#### IV. CONCLUSION

A novel, compact, chip-based RFID tag antenna boasting circularly polarized radiation characteristics has been designed, fabricated and measured for its performance. A peculiarly-fashioned, asymmetrical, asterisk-shaped design provisioned with an embedded feed line paves the way for achieving an appreciable axial ratio bandwidth of 20 MHz, as well as a minuscule footprint of  $40 \times 40 \text{ mm}^2$ , within the FCC band. Higher gain and enhanced read range have also been demonstrated when juxtaposed with other circularly polarized RFID antenna. Upon mounting on metallic surfaces, the designed tag exhibits accentuated read range making it a prime candidate for on-metal deployment.

#### ACKNOWLEDGMENT

This work was financially supported by Vinnova (The Swedish Governmental Agency for Innovation Systems) and University of Engineering and Technology Taxila, Pakistan through the Vinn Excellence Centers Program and ACTSENA Research Group Funding, respectively.

#### REFERENCES

- [1] G. Marrocco, "The art of UHF RFID antenna design: impedance-matching and size-reduction techniques," *IEEE Antennas and Propagation Magazine*, vol. 50, no. 1, pp. 66-69, 2008.
- [2] K. V. S. Rao, P. V. Nikitin, and S. F. Lam, "Antenna design for UHF RFID tags: A review and a practical application," *IEEE Transactions on Antennas and Propagation*, vol. 53, no. 12, pp. 3870-3876, 2005.
- [3] M. S. R. Bashri, M. Ibrahimy, and S. M. A. Motakabber, "Design of a wideband inductively coupled loop feed patch antenna for UHF RFID tag," *Radio Engineering*, vol. 24, no. 1, pp. 38-44, 2015.
- [4] Y. Amin, Q. Chen, L. R. Zheng, and H. Tenhunen, "Development and analysis of flexible UHF RFID antennas for "Green" electronics," *Progress in Electromagnetics Research*, vol. 130, no. 14, pp. 302-307, 2012.
- [5] E. A. Soliman, M. O. Sallam, W. L. De Raedt, and G. A. E. Vandenbosch, "Miniaturized RFID tag antenna operating in 915 MHz," *IEEE Trans. Antennas Propagat.*, vol. 11, no. 5, pp. 1068-1071, 2012.
- [6] H. W. Lui, C. F. Yang and C. H. Ku, "Novel miniature monopole tag antenna for UHF RFID applications," *IEEE Antennas and Wireless Propagation Letters*, vol. 9, pp. 363-366, 2010.
- [7] H. K. Ryu and J. M. Woo, "Miniaturisation of rectangular loop antenna using meander line for RFID tags," *IET Electronics Letters*, vol. 43, no. 7, pp. 372-374, 2007.
- [8] M. Dhaouadi, M. Mabrouk, T. P. Vuong, and A. Ghazel, "A broadband UHF tag antenna for near-field and far-field RFID communications," *Radio Engineering*, vol. 23, no. 4, pp. 1026-1032, 2014.
- [9] K. H. Lin, et al., "A loop bow-tie RFID tag antenna design for metallic objects," *IEEE Transactions on Antennas and Propagation*, vol. 61, no. 2, pp. 499-505, 2013.
- [10] S. Genovesi and A. Monorchio, "Low-profile three-arm folded dipole antenna for UHF band RFID tag mountable on metallic objects," *IEEE Antennas and Wireless Propagation Letters*, vol. 9, no. 12, pp. 1225-1228, 2010.
- [11] X. Y. Lui, Y. Liu, and M. Tentzeris, "A novel circularly polarized antenna with coin-shaped patches and a ring-shaped strip for worldwide UHF RFID applications," *IEEE Antennas and Wireless Propagation Letters*, vol. 14, pp. 574-581, 2016.
- [12] J. Shi, X. Wu, Q. Xianming, and Z. N. Chen "An omni-directional circularly polarized antenna array," *IEEE Transactions on Antennas and Propagation*, vol. 64, no. 2, pp. 574-581, 2016.
- [13] E. S. Yang, "Dual-polarized metal-mountable UHF

- RFID tag antenna for polarised diversity,” *IET Electronic Letter*, vol. 52, no. 7, pp. 496-498, 2016.
- [14] W. Choi, J. Kim, J. H. Bae, and G. Choi, “A small RFID tag antenna using proximity-coupling to identify metallic objects,” *Microwave and Optical Technology Letters*, vol. 50, no. 11, pp. 2978-2981, 2008.
- [15] P. H. Yang, Y. Li, L. J. Jiang, and T. T. Ye, “Compact metallic RFID tag antennas with a loop-fed method,” *IEEE Transactions on Antennas and Propagation*, vol. 59, no. 12, pp. 4454-4462, 2011.
- [16] T. V. Koskinen, “A thin multislotted dual patch UHF-band metal-mountable RFID tag antenna,” *Microwave and Optical Technology Letters*, vol. 53, no. 1, pp. 40-47, 2011.
- [17] T. Bjorninen, “Compact metal mountable UHF RFID tag on a barium titanate based substrate,” *Progress In Electromagnetics Research C*, vol. 26, no. 11, pp. 43-57, 2012.
- [18] Z. Wang, S. Fang, S. Fu, and S. Jia, “Single-fed broadband circularly polarized stacked patch antenna with horizontally meandered strip for universal UHF RFID applications,” *IEEE Transactions on Microwave Theory and Techniques*, vol. 59, no. 4, pp. 1066-1073, 2011.
- [19] J. Garcia, A. Arriola, F. Casado, and D. Valderas, “Coverage and readrange comparison of linearly and circularly polarised radio frequency identification ultra-high frequency tag antennas,” *IET Microwave, Antennas & Propagation*, vol. 6, no. 9, pp. 1070-1078, 2012.
- [20] H. D. Chen, S. H. Kuo, and J. L. Jheng, “Design of compact circularly polarized radio frequency identification tag antenna for metallic object application,” *Microwave and Optical Technology Letters*, vol. 55, no. 7, pp. 1481-1485, 2013.
- [21] H. D. Chen, S. H. Kuo, C. Y. D. Sim, and C. H. Tsai, “Coupling-feed circularly polarized RFID tag antenna mountable on metallic surface,” *IEEE Transactions on Antennas and Propagation*, vol. 60, no. 5, pp. 2166-2174, 2012.
- [22] Y. F. Lin, C. H. Lee, S. C. Pan, and H. M. Chen, “Proximity-fed circularly polarized slotted patch antenna for RFID handheld reader,” *IEEE Transactions on Antennas and Propagation*, vol. 61, no. 10, pp. 5283-5286, 2013.
- [23] D. M. Pozar, *Microwave Engineering*, 3<sup>rd</sup> ed., New York, NY, USA: Wiley, 2005.
- [24] G. Gonzalez, *Microwave Transistor Amplifiers: Analysis and Design*, 2<sup>nd</sup> ed., New Jersey, NJ, USA: Wiley, 1996.
- [25] S. K. Kuo, S. L. Chen, and C. T. Lin, “An accurate method for impedance measurement of RFID tag antenna,” *Progress In Electromagnetics Research*, vol. 83, pp. 93-106, 2008.
- [26] Y. Amin, Q. Chen, H. Tenhunan, and L. R. Zheng,

“Evolutionary versatile printable RFID antennas for “Green” electronics,” *Journal of Electromagnetic Waves and Applications*, vol. 26, pp. 264-273, 2012.



**Umar Hasan Khan** received his B.S. degree in Electrical Engineering from Centre for Advancement Studies in Engineering, Islamabad in the year 2009, and his M.S. degree is in Electrical Engineering from National University of Science and Technology in the year 2013.

He joined the University of Engineering and Technology, Taxila the same year as a full-time Ph.D. Researcher, where he is working towards his doctoral degree focused on miniaturized RFID antennas for IoT.



**Bilal Aslam** received his B.S. degree in Electrical Engineering from the University of Engineering and Technology, Taxila in the year 2007, and his M.S. degree in Electrical Engineering from National University of Science and Technology in the 2013. The same

year, he joined the University of Engineering and Technology, Taxila as a full-time Ph.D. Researcher, where he is pursuing his doctoral degree focused on RFID antennas for biomedical applications.



**Humayun Shahid** received his B.S. degree in Communication Systems Engineering from Institute of Space Technology, Islamabad in the year 2008, and his M.S. degree in Signal Processing from Nanyang Technological University, Singapore in the year 2011. His current research

interests include antenna design, microwave engineering and RFID technology. He currently serves as an Assistant Professor and Director of Postgraduate Studies at the Telecommunication Engineering Department, University of Engineering and Technology, Taxila.



**Muhammad Awais Azam** received his Ph.D. degree in Pervasive and Ubiquitous Computing from London, UK in 2012. He is working as an Assistant Professor at the Department of Computer Engineering, UET Taxila, Pakistan. He leads a research team of M.S. and Ph.D.

students in the area of Pervasive and Ubiquitous Computing. His research interest includes network architecture, communication protocols, network security, embedded systems, ambient intelligence, wireless communications, opportunistic networks and recommender systems.



**Yasar Amin** is Chairman and Associate Professor of Telecommunication Engineering Department, University of Engineering and Technology Taxila, Pakistan. He is founder of ACTSENA Research Group at UET Taxila, Pakistan. He has done his B.Sc. in Electrical

Engineering in 2001 with specialization in Telecommunication and M.Sc. in Electrical Engineering in 2003 with specialization in System-on Chip Design from Royal Institute of Technology (KTH), Sweden. His Ph.D. is in Electronic and Computer Systems from Royal Institute of Technology (KTH), Sweden, with research focus on printable green RFID antennas for embedded sensors, while has MBA in Innovation and Growth from Turku School of Economics, University of Turku, Finland. He has done several specialized courses from Stanford University, California, USA and Massachusetts Institute of Technology (MIT), USA. He has supervised over 15 M.Sc. thesis, and presently supervising 8 doctoral thesis. He is presently serving as leading Guest Editor at two International Journals and an active Reviewer of more than a dozen well reputed International journals. He has contributed to over 20 journal papers, over 30 reviewed international conference papers. Yasar is a Member of IEEE, IET, ACM and ACES.



**Hannu Tenhunen** is Chair Professor of Electronic Systems at Royal Institute of Technology (KTH), Stockholm, Sweden. Tenhunen has held Professor positions as Full Professor, Invited Professor or Visiting Honorary Professor in Finland (TUT, UTU), Sweden

(KTH), USA (Cornell U), France (INPG), China (Fudan and Beijing Jiatong Universities), and Hong Kong (Chinese University of Hong Kong), and has an Honorary Doctorate from Tallinn Technical University. He has been Director of multiple national large scale

research programs or being an Initiator and Director of national or European graduate schools. He has actively contributed on VLSI and SoC design in Finland and Sweden via creating new educational programs and research directions, most lately at European level as being the EU-level Education Director of the new European flagship initiative European Institute of Technology and Innovations (EIT), and its Knowledge and Innovation Community EIT ICT Labs.

Tenhunen has been active in promoting the innovation system and innovation support mechanism in research and education both at national and European level. Tenhunen has been a board member in science parks, start-up companies, and has served as Advisor or Expert for high technology companies and venture capitalists, as well as Evaluator for EU and national programs and research institutes. He has supervised over 70 M.Sc. thesis, 39 doctoral thesis, and 8 post-doc. From his doctoral students and post-docs, as of today, 21 are currently professors and associate professors. Tenhunen has served in Technical Program Committees of all major conferences in his area, have been General Chairman or Vice-Chairman or Member of Steering Committee of multiple conferences in his core competence areas. He has been one of the founding editorial board member of 3 scientific journal, have been Guest Editor for multiple special issues of scientific journals or books, and have contributed numerous invited papers to journals. He has contributed to over 110 journal papers, over 625 reviewed international conference papers, over 170 non-reviewed papers, local conference papers, or other publications, and 9 international patents granted in multiple countries. Tenhunen is Member of Academy of Engineering Science of Finland.